

## Chronological data for the Middle Miocene to Pliocene sequence around the southwestern Sendai Plain, with special reference to the uplift history of the Ou Backbone Range

Osamu Fujiwara<sup>1</sup>, Yukio Yanagisawa<sup>2</sup>, Toshiaki Irizuki<sup>3</sup>, Masanori Shimamoto<sup>4</sup>, Hiroki Hayashi<sup>5</sup>, Tohru Danhara<sup>6</sup>, Keisuke Fuse<sup>7</sup> and Hideki Iwano<sup>8</sup>

Osamu Fujiwara, Yukio Yanagisawa, Toshiaki Irizuki, Masanori Shimamoto, Hiroki Hayashi, Tohru Danhara, Keisuke Fuse and Hideki Iwano (2008) Chronological data for the Middle Miocene to Pliocene sequence around the southwestern Sendai Plain, with special reference to the uplift history of the Ou Backbone Range. *Bull. Geol. Surv. Japan*, vol. 59 (7/8), 423-438, 7 figs., 2 tables.

**Abstract:** Middle Miocene to Pliocene chronostratigraphic data were obtained from three sections on the southwestern margin of the Sendai Plain, northeast Japan. In this tectonically active area, we newly infer the numerical age of the coastal sedimentary sequence on the basis of 27 fission track ages in combination with planktonic foraminiferal and diatom analyses. The Hatatate Formation cropping out along the Natori-gawa Section approximately ranges from 13 Ma to 11.5 Ma in age. The Tsunaki Formation ranges from 10 Ma to 8.3 Ma, and the basal part of the Nashino Formation is assigned to 6.4 Ma. Four major unconformities were recognized in the Middle Miocene to Pliocene sequence in the study area from a compilation of chronological data: ca. 9 Ma, 6.4Ma, latest Miocene, and 3.5Ma, respectively. The oldest unconformity was newly identified in this study. Formative timings of these unconformities correlate well with the uplift history of the Ou Backbone range reconstructed by Nakajima *et al.* (2006). These data provide a restriction to reconstruct the uplift history of the Northeast Honshu Arc.

**Keywords:** biostratigraphy, fission track age, Miocene, northeast Honshu Arc, Pliocene, Sendai, Tsunaki Formation, Hatatate Formation, unconformity, uplift history

### 1. Introduction

The Miocene and later sedimentary sequence exposed around the Sendai area represents Neogene shallow marine and coastal litho- and biostratigraphies along the Pacific side (fore-arc side) of northeast Japan (Fig. 1A). The sequence consists mainly of sandy and muddy sediments and yields various kinds of micro- and macro-fossils of terrestrial and marine origin. Abundant pyroclastics derived from the backbone range located west of the Sendai area also characterize the Neogene sequence.

Studies of these deposits based on litho- and biostratigraphic criteria have revealed a complicated geological history for the Northeast Honshu Arc that was controlled by eustatic sea-level changes and active tectonic movements relating to subduction of the Pacific plate

along the Japan Trench (*e.g.* Sato, 1994). In particular, these studies make clear that the tectonic history of the late Middle Miocene to Pliocene is a key to understand the tectonic and biological evolution of NE Japan, because major unconformities, indicative of regional uplift, are recognized for this period (*e.g.* Nakajima *et al.*, 2006).

Accurate dating of the Middle Miocene to Pliocene sequence around the Sendai area is required to solve persistent problems. However, chronologic data are still insufficient both in radiometric and biostratigraphic studies. The present study provides newly obtained fission track (FT) ages and planktonic foraminiferal and diatom biohorizons for the Middle Miocene to Pliocene sequence around the southwestern Sendai Plain. On the basis of these age data, we will estimate the formation

<sup>1</sup>Active Fault Research Center, National Institute of Advanced Industrial Science and Technology (AIST), 1-1-1 Higashi, Tsukuba 305-8567, Japan

<sup>2</sup>Institute of Geology and Geoinformation, National Institute of Advanced Industrial Science and Technology (AIST), 1-1-1 Higashi, Tsukuba 305-8567, Japan

<sup>3,5</sup>Department of Geoscience, Interdisciplinary Faculty of Science and Engineering, Shimane University, 1060 Nishikawatsu, Matsue 690-8504, Japan

<sup>4</sup>The Tohoku University Museum, Aobayama, Aoba-ku, Sendai 980-8578, Japan

<sup>6,8</sup>Kyoto Fission-Track Co. Ltd., 44-4 Minamitajiri-cho, Omiya, Kita-ku, Kyoto 603-8832, Japan

<sup>7</sup>Kamisugi, Aoba-ku, Sendai 980-0011, Japan

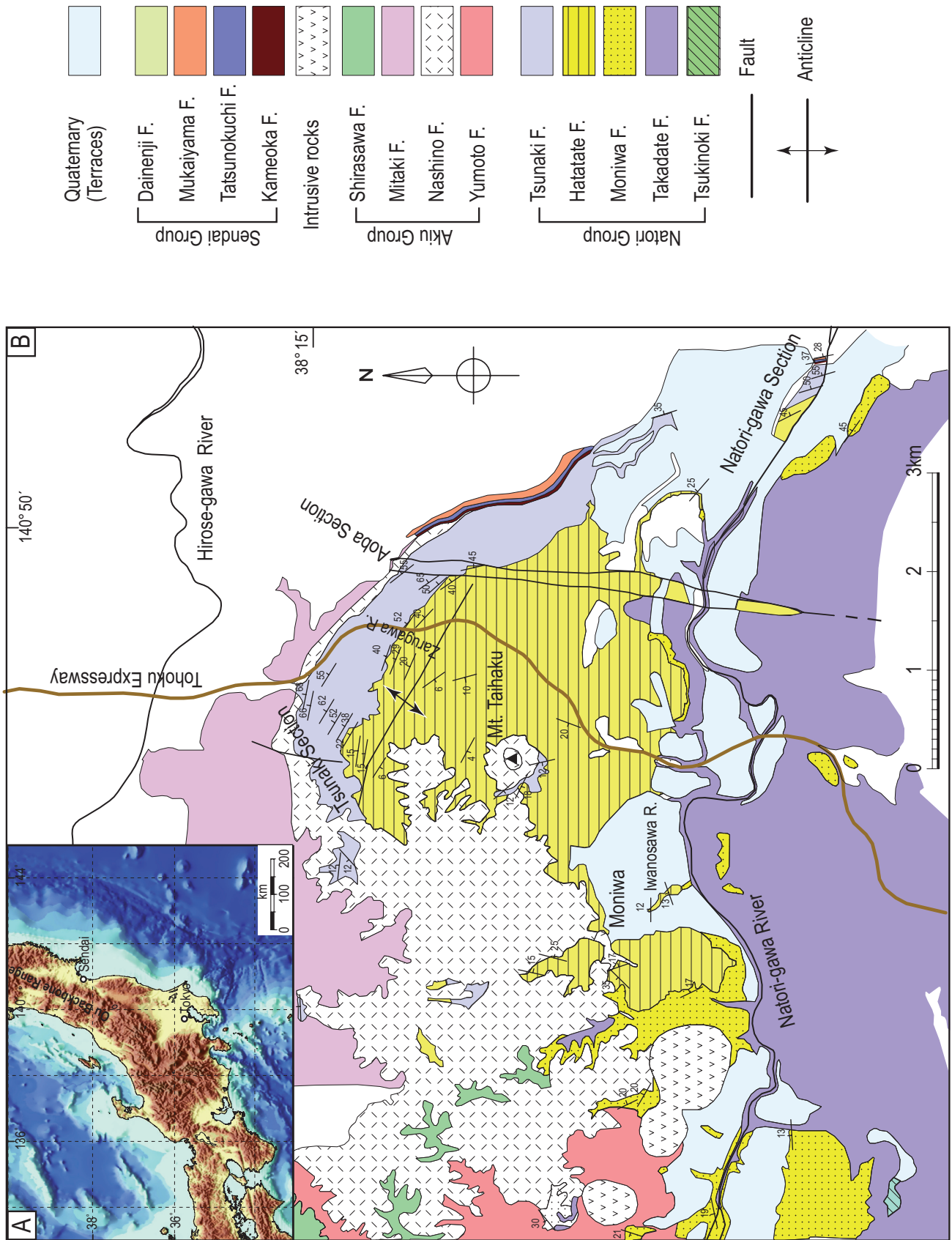


Fig. 1 Index map. A: Northeast Honshu Arc and study area. B: Geological map of study area (Kitamura *et al.*, 1986, partly modified).

ages of unconformities recognized in this sedimentary sequence and correlate them with the unconformities distributed in back-arc region of Northeast Honshu Arc.

## 2. Study area

The study area is located in the southwestern margin of the Sendai Plain (Fig. 1B). The area consists of a western hilly region and an eastern lowland, in general. Most of the hilly region consists of Miocene and later sedimentary rocks. Many outcrops are distributed along the rivers and valleys incising the hilly region.

A Middle to Late Miocene sequence exposed in the hilly region, the Moniwa-Tsunaki area (Fig. 1B), including the type section of some formations has been well studied. Biostratigraphic data are available, such as planktonic foraminifers, calcareous nannofossils, radiolarians and diatoms (*e.g.* Oda *et al.*, 1984; Yanagisawa, 1999; Shimamoto *et al.*, 2001; Yanagisawa and Hayashi, 2003) from this area. On the other hand, few chronostratigraphic data have been reported from the eastern region, the Natori-gawa area (Fig. 1B), though a Middle Miocene to Pliocene sequence is continuously exposed along the Natori-gawa River.

## 3. Stratigraphy

The Miocene and later sequence distributed in the study area has been divided into three groups, the Natori, Akiu and Sendai Groups, in ascending order (Fig. 2).

### 3.1 Natori Group

The Natori Group unconformably overlies pre-Tertiary granitic and sedimentary rocks (Kitamura *et al.*, 1986) and is composed of the Tsukinoki, Takadate, Moniwa, Hatatate and Tsunaki Formations, in ascending order (Fig. 2). The first two formations are mainly composed of lacustrine sedimentary and volcanic rocks, and range from Early to Middle Miocene in age (Kitamura *et al.*, 1986). The last three formations consist of marine sedimentary rocks.

The Moniwa Formation partially interfingers with the Takadate Formation (Kitamura *et al.*, 1986) and mainly consists of rocky and sandy coastal deposits. It is assigned to planktonic foraminiferal zone N.8 of Blow (1969) (*e.g.* Kitamura *et al.*, 1986) and calcareous nannofossil zones CN3-CN4 of Okada and Bukry (1980) (Oda *et al.*, 1984). The Moniwa Formation ranges from 20 to 80 m in thickness.

The Hatatate Formation conformably overlies the Moniwa Formation and is about 140 m in thickness. It mainly consists of mudstone and muddy sandstone deposited in an open marine environment at a depth of around 50 m (Ogasawara and Masuda, 1989). Acidic tuff layers (Htt 8-31) that can be widely traced in the

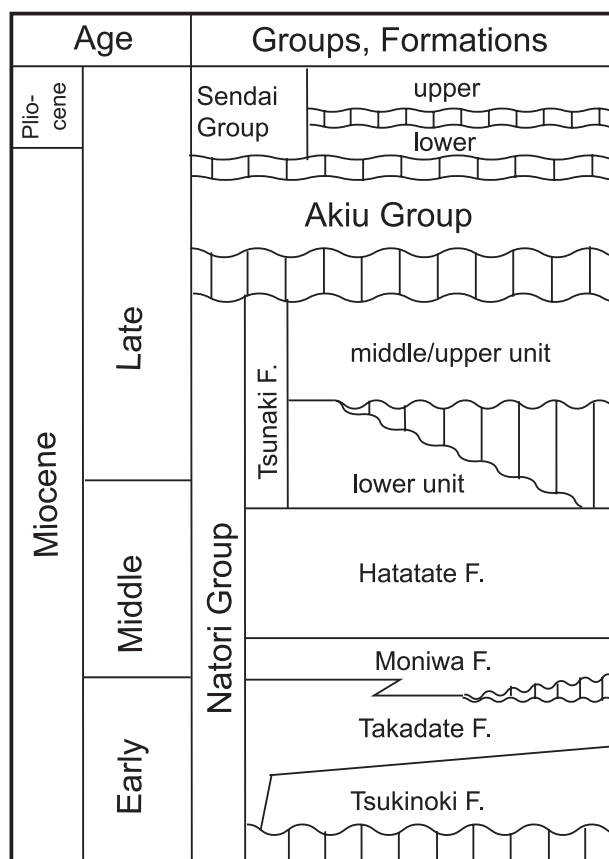


Fig. 2 General stratigraphy around the study area

study area are intercalated in this formation (Shimamoto *et al.*, 2001). The formation represents a transgressive stage in Northeast Japan during the late Middle Miocene. According to biostratigraphic studies, the Hatatate Formation ranges in time about 15 to 11 Ma (*e.g.* Shimamoto *et al.*, 2001).

The Tsunaki Formation conformably covers the Hatatate Formation around their type section. It is composed of alternating beds of sandstone, conglomerate and tuff. The total thickness of the Tsunaki Formation attains a maximum of more than 350 m. Osozawa (2002) recognized 70 key beds, including tuff beds and conglomerate beds, from the formation. No chronologic data has been obtained from the Tsunaki Formation. The Tsunaki Formation unconformably covers the Hatatate Formation in the Natori-gawa Section, as mentioned below.

### 3.2 Akiu Group

The Akiu Group unconformably covers the Natori Group and is mainly composed of terrestrial volcanic and pyroclastic materials, including thick pumice tuff beds and tuff breccia beds, supplied by intense volcanism that occurred in the Late Miocene (Kitamura *et al.*, 1986). The Akiu Group reaches 200 m or more in thickness (Kitamura *et al.*, 1986).

### 3.3 Sendai Group

The Sendai Group unconformably covers underlying formations and is a representative of the latest Miocene to Pliocene sequence on the Pacific side of Northeast Japan. The group is divided into lower and upper parts by a regional unconformity. The lower part consists of the Kameoka and Tatsunokuchi Formations and the upper part consists of the Mukaiyama and Dainenji Formations. The total thickness of the Sendai Group is about 100 m in the study area (Kitamura *et al.*, 1986).

The Kameoka Formation is composed of conglomerate, sandstone and siltstone with interbedded lignite. The Tatsunokuchi Formation consists of alternation of siltstone, sandstone and tuff that were deposited in a large shallow bay. The formation is known for yielding various kinds of plant and animal fossils, including some mammals. The Mukaiyama Formation unconformably covers the Tatsunokuchi Formation and consists of alternation of conglomerate, sandstone, siltstone, tuff and lignite. The Hirosegawa Tuff Member, consisting of thick pumice flow deposits, is intercalated in the lower part of the formation. Danhara and Iwano (1995) reported the FT ages of  $3.5 \pm 0.4$  Ma from the Hirosegawa Tuff Member. The Dainenji Formation consists mainly of alternating beds of sandstone and siltstone with tuff beds. The formation yields plant and animal fossils including mollusks and mammals (*e.g.* Kitamura *et al.*, 1986).

According to the diatom biostratigraphy and magnetostratigraphy, the Kameoka and Tatsunokuchi formations range from latest Miocene to Early Pliocene in age, and the Mukaiyama and Dainenji formations range from Early to Late Pliocene (Yanagisawa, 1990).

## 4. Materials

Samples analyzed were collected from outcrops in the Tsunaki, Aoba and Natori-gawa Sections in Fig.1B. Samples for fission track dating were collected from the three sections. Samples for planktonic foraminiferal and diatom analysis were taken from the Natori-gawa Section.

### 4.1 Tsunaki Section

This section is located at the type locality of the Tsunaki Formation (Fig. 1B and Fig. 3). Outcrops are intermittently distributed along a small river and its tributaries. The Tsunaki Formation is roughly divided into three units; lower, middle and upper units (Fig. 4). The lower unit is mainly composed of alternating beds of pumice tuff, lapilli tuff and tuffaceous sandstone. The middle unit mainly consists of well sorted tuffaceous fine-grained sandstone that yields fossil mollusks implying inner shelf conditions. The unit intercalates pumice tuff beds, fine tuff beds and graded conglomerate beds. A pebble conglomerate bed at the base of the unit, the

key bed 57 of Osozawa (2002), can be widely traced in the study area. The upper unit is mainly composed of alternating beds of lapilli tuff, pumice tuff, conglomerate and tuffaceous sandstone. Black-colored siltstone alternating with thin lapilli tuff layers characterizes the basal part of the unit. One sample for FT dating was taken from the lower part of the middle unit (Fig. 4).

### 4.2 Aoba Section

This section, consisting of cliffs along a small valley and artificial cuts for an athletic field, is located about 2 km east of the Tsunaki Section (Fig. 1B and Fig. 3). The Tsunaki Formation and the lower part of the Nashino Formation can be observed in this section. Lithofacies of the Tsunaki Formation in present section is closely similar to that of the Tsunaki Section. The Nashino Formation consists mainly of alternating beds of tuffaceous sandstone, pumice tuff and fine tuff.

A total of eight samples for FT dating were collected from the present section, seven from the Tsunaki Formation and one from the Nashino Formation (Figs. 3 and 4).

### 4.3 Natori-gawa Section

This section is located along the lower reaches of the Natori-gawa River (Figs 1B and Fig. 5). A sedimentary sequence extending from the Hatatate Formation to the Dainenji Formation almost continuously crops out along the river bed. Outcrops are exposed for about 1 km in a dip-normal direction and up to 100 m along their strike. The dip of the beds gradually decreases from the western end of the section (about 45°) to the eastern end (20–10°). The total thickness of the sequence is about 370 m. Outcrops were leveled to make the 1/2500-scale geological map (Fig. 5).

The Hatatate Formation is roughly divided into lower and upper units in this section (Fig. 6). The lower unit, beneath the 146-m-level in Fig.6, is mainly composed of alternating beds of siltstone and fine- to medium-grained sandstone, and intercalates with calcareous sandstone beds. This unit shows a coarsening-upward trend as a whole. The upper unit, from the 146-m to 200-m-level in Fig.6, has a basal conglomerate bed and mainly consists of siltstone and fine-grained sandstone. The upper unit also shows a coarsening upward trend as a whole. The Hatatate Formation intercalates many pumice tuff beds and fine tuff beds, NTR-1 to 37 and yields fossils of mollusks and brachiopods.

The Tsunaki Formation occupies the middle part of the Natori-gawa Section, from the 200-m to 284-m level in Fig.6. It unconformably covers the Hatatate Formation with a basal conglomerate bed. The lower part of the Tsunaki Formation in the present section, beneath 260-m level in Fig.6, shows closely similar lithological character to that of the middle part of the Tsunaki Formation in the Tsunaki and Aoba Sections. It intercalates tuff beds



Fig. 3 Map showing the Tsunaki and Aoba Sections, modified from the 1/25,000-scale topographic map “Sendai seinanbu” and “Sendai seihokubu,” Geographical Survey Institute.

NTR-38 to 49. The upper part of the Tsunaki Formation, from the 260-m to 284-m level in Fig. 6, is characterized by much coarser sediments than the lower part. Cross-stratified tuffaceous medium- to coarse-grained sandstone and conglomerate beds mainly comprise the upper part of the Tsunaki Formation. Tuff beds NTR-50 to 55 are intercalated in the upper part of the Tsunaki Formation.

The Kameoka Formation mainly consists of siltstone and cross-bedded sandstone and intercalates lignite beds. The Tatsunokuchi Formation consists of bioturbated mudstone and sandstone and intercalates fine-grained tuff beds (NTR-62 and 63). The Mukaiyama Formation is mainly composed of alternating beds of mudstone, cross-bedded sandstone and acidic tuff (NTR-64 to 70) with the intercalation of lignite beds. The Hirosegawa Tuff Member (NTR-65) is intercalated in the lower part of the Mukaiyama Formation. The Dainenji Formation is composed of bioturbated mudstone and fine-grained sandstone and intercalates a pumice tuff bed (NTR-71).

A total of 18 samples for FT dating were collected from the Natori-gawa section, seven samples from the Hatatate Formation, eight samples from the Tsunaki Formation, two samples from the Mukaiyama

Formation and one sample from the Dainenji Formation (Figs. 5 and 6).

A total of 95 samples for planktonic foraminiferal analysis were taken from the Hatatate (NM-1 to 43, NH-1 to 47) and Tsunaki (NT-1 to 5) formations (Figs. 5 and 6). Twenty-four samples for diatom analysis were taken from the upper unit of the Hatatate Formation, from the 147-m to 194-m level in Fig. 6, at even intervals.

## 5. Methods

### 5.1 Fission track dating

Samples were selected mainly from pumice tuff and acidic tuff that shows relative high purity. The homogeneity of the zircon crystals was checked based on their morphological characteristics, such as color and shape, and information on spontaneous track density and track length distributions prior to dating. FT ages were determined using the external detector method that applies to external surfaces of zircon (ED2 method; Danhara, *et al.*, 1991) and were calibrated using the zeta approach (Hurford, 1990, a, b). Further procedures and experimental conditions are shown in detail by Danhara *et al.* (1991, 2003).

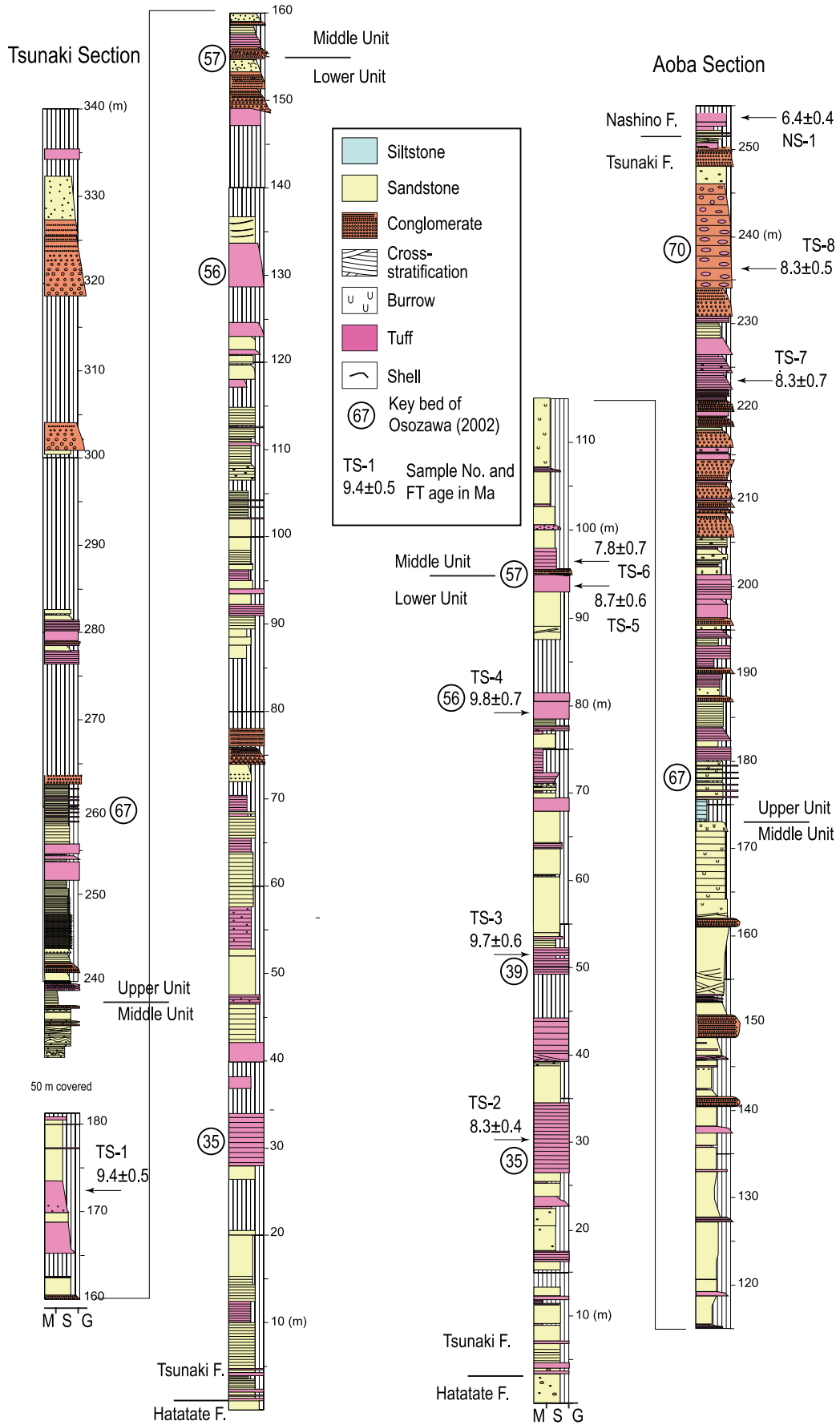


Fig. 4 Columnar sections of the Tsunaki and Aoba Sections

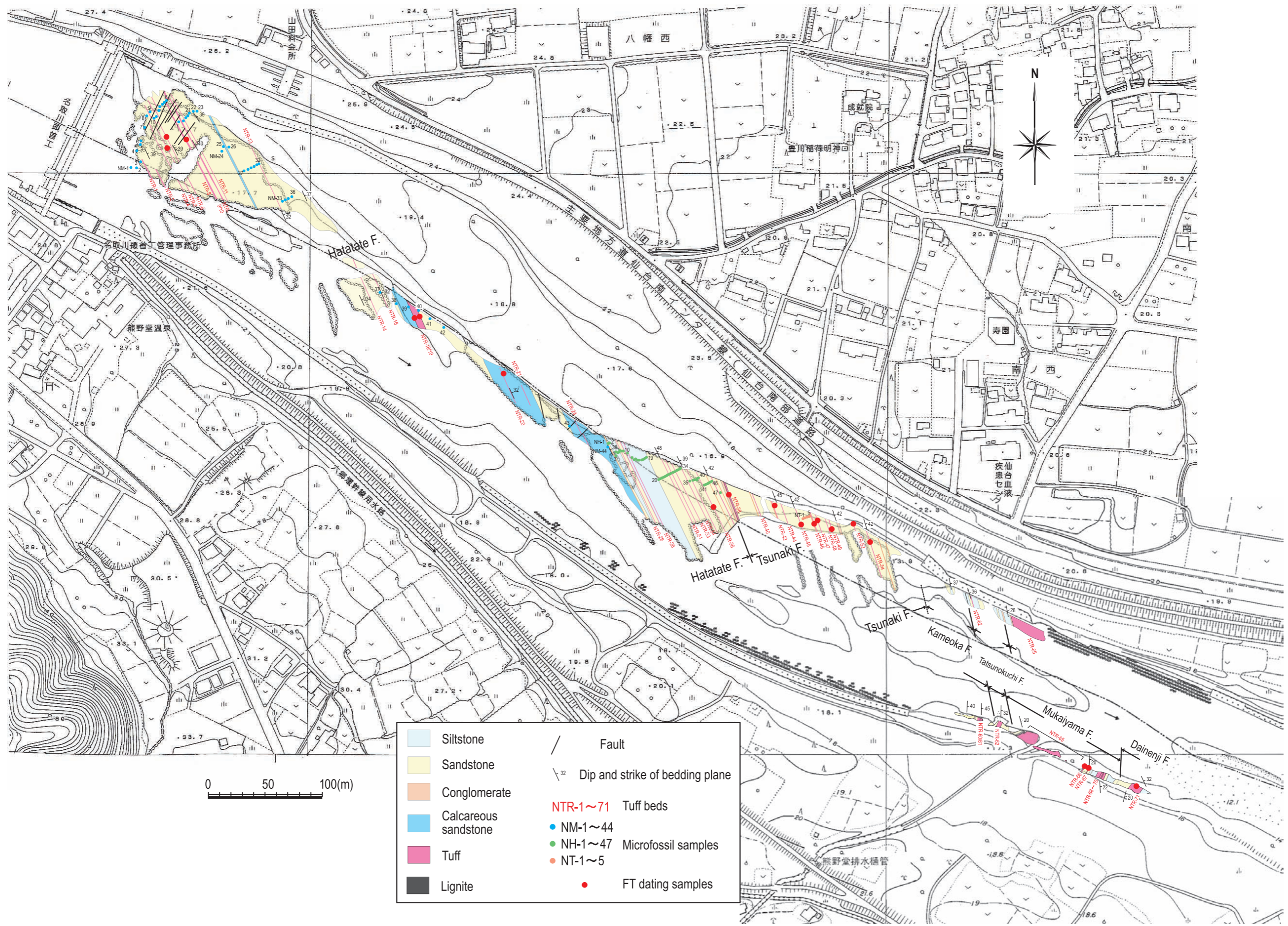


Fig. 5 Geological map of the Natori-gawa Section. 1/2500-scale topographic map of Sendai City was used as base map.

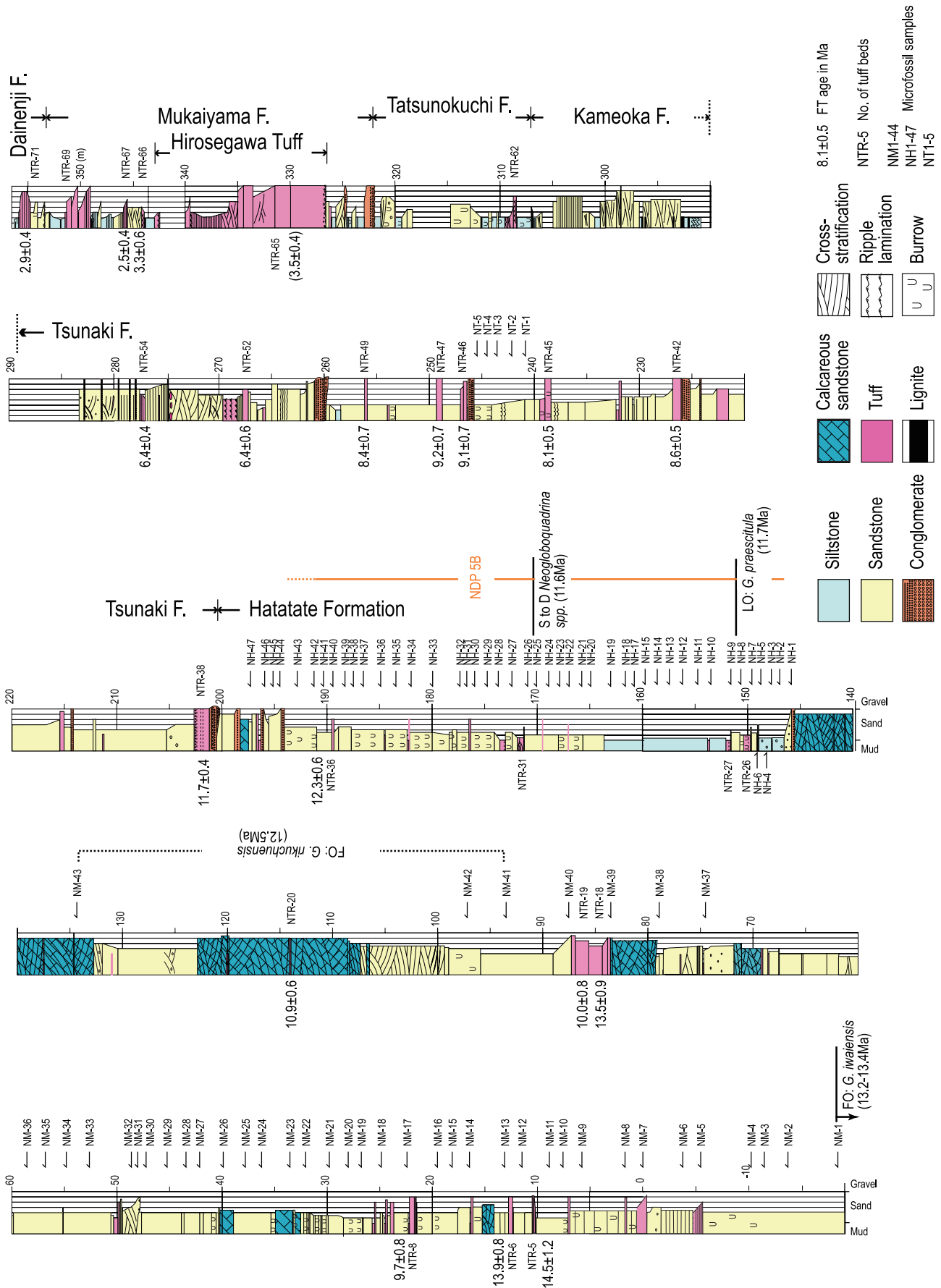


Fig. 6 Columnar sections of the Natori-gawa Section.



Thirty grains from each sample were measured for dating. Some data failed the  $\chi^2$ -test (Galbraith, 1981), due to the mixture of crystals with extremely old ages. In that case, we excluded the older grains as being detrital, and grains that passed the  $\chi^2$ -test were used to determine the FT age of the sample. As a result, 25-30 grains were used to calculate the FT age for each sample, with the exception of samples NTR-66 (8 grains) and NTR-71 (18 grains).

### 5.2 Planktonic foraminifera analysis

Rock samples were disaggregated with the use of a sodium sulfate solution and naphtha. Planktonic foraminiferal specimens were picked from residues coarser than 125 micrometer.

### 5.3 Diatom analysis

The samples were prepared following the method of Akiba (1986). A strewn slide for light microscopy (LM) was prepared for each sample on an 18 x 18 mm cover glass and mounted in Pleurax on a glass slide.

## 6. Results

### 6.1 FT ages

Fission track data are shown in Tables. 1 and 2.

#### Tsunaki Section

The calculated age of Sample TS-1 is  $9.4 \pm 0.5$  Ma. The sample was taken from the lower part of the middle unit of the Tsunaki Formation (Fig. 4), about 15 m above key bed 57 of Osozawa (2002).

#### Aoba Section

Four FT ages,  $8.3 \pm 0.4$  Ma,  $9.7 \pm 0.6$  Ma,  $9.8 \pm 0.7$  Ma,  $8.7 \pm 0.6$  Ma, in ascending order, were calculated for the samples from the lower unit of the Tsunaki Formation (Fig. 4). An FT age of  $7.8 \pm 0.7$  Ma was calculated for Sample TS-6 at the basal part of the middle unit of the Tsunaki Formation. Two FT ages,  $8.3 \pm 0.7$  Ma and  $8.3 \pm 0.5$  Ma were calculated for samples from the upper unit of the Tsunaki Formation. An FT age of  $6.4 \pm 0.4$  Ma was calculated for sample NS-1 from the basal part of the Nashino Formation (Fig. 4).

#### Natori-gawa Section

Calculated FT ages are shown in Figs. 6 and 7. A total of seven FT ages were calculated for samples from the Hatatate Formation and they were classified into two groups, a younger age group and an older age group. The former group includes samples NTR-8 ( $9.7 \pm 0.8$  Ma), NTR-19 ( $10.0 \pm 0.8$  Ma) and NTR-20 ( $10.9 \pm 0.6$  Ma). The latter group includes samples NTR-5 ( $14.5 \pm 1.2$  Ma), NTR-6 ( $13.9 \pm 0.8$  Ma), NTR-18 ( $13.5 \pm 0.9$  Ma) and NTR-36 ( $12.3 \pm 0.6$  Ma).

FT ages from the Tsunaki Formation were also classified into two groups, younger and older, with the exception of sample NTR-38. The former group includes five samples distributed around 8.5 Ma, and they were

obtained from the lower part of the formation. The latter group comprised of two samples,  $6.4 \pm 0.6$  Ma and  $6.4 \pm 0.4$  Ma, and obtained from the upper part of the formation. Sample NTR-38 from a pumice tuff bed at the basal part of the Tsunaki Formation shows an exceptionally old age of  $11.7 \pm 0.4$  Ma. Sample NTR-38 mainly consists of rounded pumice, and is regarded as reworked material.

Two FT ages,  $3.3 \pm 0.6$  Ma and  $2.5 \pm 0.4$  Ma, were calculated from the samples from the Mukaiyama Formation. Sample NTR-71 from the Dainenji Formation shows an FT age of  $2.9 \pm 0.4$  Ma.

### 6.2 Planktonic foraminifers

Planktonic foraminifers were found in samples NM-1 to NH-41 of the Natori-gawa Section (Fig. 6). Fossil preservation is generally poor owing to weathering of shell surface structures or accretion of sand grains. Five biohorizons are detected as follows, in ascending order: *Globorotalia iwaiensis* Takayanagi and Oda is contained successively from the lowest sample NM-1 and upwards, thus the first occurrence (FO) of this species should be located below the lowermost sample in this study. *Globorotalia rikuchensis* Takayanagi and Oda abundantly occurs from sample NM-43 and upwards. We considered the FO of *G. rikuchensis* between samples NM-40 and NM-43 because samples NM-41 and NM-42 yielded few planktonic foraminifers. The last occurrence (LO) of *Globorotalia praescitula* Blow was recognized between samples NH-8 and NH-9. The dominant coiling direction change from sinistral to dextral (S to D) in *Neogloboquadrina* spp. (*N. continuosa*, *N. mayeri*, and *N. pseudopachyderma*) was detected between samples NH-25 and NH-26. The LO of *N. mayeri* should be placed above sample NH-41.

Four of the above five biohorizons were also found in the type locality of the Hatatate Formation, around the Moniwa area in Fig. 1B (Shimamoto *et al.*, 2001). The FO of *G. iwaiensis* was recognized at the lowest part of the Hatatate Formation. The FO of *G. rikuchensis* was detected within the lower part of the Hatatate Formation in the Iwanosawa section (Fig. 1B). The LO of *G. praescitula* was placed at the middle part of the Hatatate Formation. The S to D of *Neogloboquadrina* spp. was detected in the upper part of the Hatatate Formation in the Zarugawa section (Fig. 1B). Accordingly, the present interval including the NM and NH samples should be correlated with the Hatatate Formation of the type locality according to planktonic foraminiferal data.

The FO of *G. rikuchensis* was numerically estimated to be 12.5 Ma by direct correlation with diatom ages in the Ichinoseki area, about 90 km northward of the present area (Yanagisawa, 1999; Yanagisawa and Hayashi, 2003). In addition, each numerical age of the FO of *G. iwaiensis*, LO of *G. praescitula* and S to D of *Neogloboquadrina* spp. were determined to be 13.2-13.4

Table 1 Fission track data from the samples collected from the Tsunaki and Aoba Sections.

Sample code	No. of crystals	Spontaneous		Induced		Dosimeter		P( $\chi^2$ ) (%)	U-content (ppm)	Age in Ma ( $\pm 1\sigma$ )	
		$\rho_s$ (cm <sup>-2</sup> )	$N_s$	$\rho_i$ (cm <sup>-2</sup> )	$N_i$ ( $\times 10^6$ cm <sup>-2</sup> )	$\rho_d$ ( $\times 10^4$ cm <sup>-2</sup> )	$N_d$				$r$
TS-1	25	$9.28 \times 10^5$	428	$2.89 \times 10^6$	1330	8.394	4297	0.685	35	320	<b>9.4</b> $\pm$ <b>0.5</b>
TS-2	29	$1.16 \times 10^6$	858	$3.92 \times 10^6$	2909	8.046	4120	0.830	0	410	<b>8.3</b> $\pm$ <b>0.4</b>
TS-3	28	$9.81 \times 10^5$	351	$2.84 \times 10^6$	1017	8.051	4122	0.948	39	290	<b>9.7</b> $\pm$ <b>0.6</b>
TS-4	29	$1.02 \times 10^6$	280	$2.95 \times 10^6$	808	8.060	4127	0.694	8	300	<b>9.8</b> $\pm$ <b>0.7</b>
TS-5	30	$1.29 \times 10^6$	308	$4.18 \times 10^6$	994	8.069	4131	0.918	84	430	<b>8.7</b> $\pm$ <b>0.6</b>
TS-6	30	$2.79 \times 10^5$	173	$1.05 \times 10^6$	648	8.386	4294	0.543	45	120	<b>7.8</b> $\pm$ <b>0.7</b>
TS-7	27	$7.50 \times 10^5$	180	$2.78 \times 10^6$	666	8.826	4519	0.693	9	260	<b>8.3</b> $\pm$ <b>0.7</b>
TS-8	28	$9.57 \times 10^5$	467	$2.91 \times 10^6$	1419	7.248	3711	0.822	20	380	<b>8.3</b> $\pm$ <b>0.5</b>
NS-1	30	$3.92 \times 10^5$	468	$1.54 \times 10^6$	1842	7.252	3713	0.463	11	200	<b>6.4</b> $\pm$ <b>0.4</b>

(1)  $\rho$  and  $N$  are the density and total number of fission tracks counted, respectively.

(2) All samples were analysed by the external detector method (ED2) that applies to external surfaces of zircon (Danbara *et al.*, 1991).

(3) Ages were calculated using a dosimeter glass NIST-SRM612, and age calibration factors  $\zeta=350\pm 3$  of T. Danbara (Danbara *et al.*, 2003) for samples TS1-5 and  $347\pm 3$  of H. Iwano (Danbara *et al.*, 2003) for samples TS-6-8 and NS-1.

(4)  $P(\chi^2)$  is the probability of obtaining the  $\chi^2$ -value for  $v$  degrees of freedom (where  $v$ = number of crystals-1).

(5)  $r$  is correlation coefficient between  $\rho_s$  and  $\rho_i$ .

(6) Zircon crystals were irradiated using the pneumatic tube of reactor unit JRR-4 at the Japan Atomic Energy Research Institute (JAERI), Japan.

Table 2 Fission track data from the samples collected from the Natori-gawa Section.

Sample code	No. of crystals	Spontaneous		Induced		Dosimeter		$r$	P( $\chi^2$ ) (%)	U-content (ppm)	Age in Ma ( $\pm 1\sigma$ )
		$\rho_s$ (cm <sup>-2</sup> )	$N_s$	$\rho_i$ (cm <sup>-2</sup> )	$N_i$	$\rho_d$ ( $\times 10^4$ cm <sup>-2</sup> )	$N_d$				
NTR-5	30	3.63 $\times 10^5$	225	7.67 $\times 10^5$	476	8.766	4488	0.983	79	70	14.5 $\pm$ 1.2
NTR-6	29	1.28 $\times 10^6$	550	2.81 $\times 10^6$	1208	8.762	4486	0.936	88	270	13.9 $\pm$ 0.8
NTR-8	29	5.31 $\times 10^5$	241	1.37 $\times 10^6$	624	7.223	3698	0.804	27	180	9.7 $\pm$ 0.8
NTR-18	30	4.42 $\times 10^5$	340	1.01 $\times 10^6$	775	8.785	4498	0.764	46	100	13.5 $\pm$ 0.9
NTR-19	25	3.62 $\times 10^5$	238	9.06 $\times 10^5$	595	7.227	3700	0.794	9	120	10.0 $\pm$ 0.8
NTR-20	25	1.29 $\times 10^6$	560	3.63 $\times 10^6$	1577	8.794	4503	0.885	5	340	10.9 $\pm$ 0.6
NTR-36	26	1.25 $\times 10^6$	647	3.12 $\times 10^6$	1611	8.776	4493	0.837	5	300	12.3 $\pm$ 0.6
NTR-38	29	1.13 $\times 10^6$	1250	2.96 $\times 10^6$	3287	8.771	4491	0.930	8	280	11.7 $\pm$ 0.4
NTR-42	29	8.05 $\times 10^5$	458	2.89 $\times 10^6$	1646	8.799	4505	0.921	97	270	8.6 $\pm$ 0.5
NTR-45	30	6.81 $\times 10^5$	314	2.11 $\times 10^6$	972	7.240	3707	0.799	17	270	8.1 $\pm$ 0.5
NTR-46	30	4.73 $\times 10^5$	235	1.31 $\times 10^6$	651	7.235	3705	0.867	81	170	9.1 $\pm$ 0.7
NTR-47	30	6.73 $\times 10^5$	267	2.26 $\times 10^6$	898	8.803	4507	0.859	94	210	9.2 $\pm$ 0.7
NTR-49	29	6.14 $\times 10^5$	179	2.26 $\times 10^6$	660	8.808	4510	0.887	98	210	8.4 $\pm$ 0.7
NTR-52	30	3.61 $\times 10^5$	161	1.41 $\times 10^6$	629	7.231	3702	0.674	46	180	6.4 $\pm$ 0.6
NTR-54	29	4.52 $\times 10^5$	299	1.98 $\times 10^6$	1309	8.041	4117	0.898	36	200	6.4 $\pm$ 0.4
NTR-66	8	2.21 $\times 10^5$	33	1.97 $\times 10^6$	294	8.379	4290	0.729	55	220	3.3 $\pm$ 0.6
NTR-67	29	1.19 $\times 10^5$	51	1.38 $\times 10^6$	590	8.372	4286	0.382	71	160	2.5 $\pm$ 0.4
NTR-71	18	1.32 $\times 10^5$	65	1.30 $\times 10^6$	642	8.365	4283	0.869	74	150	2.9 $\pm$ 0.4

Same notes as Table 1.

Calibration factors used are  $\zeta = 350 \pm 3$  of T. Danhara for samples NTR-5, 6, 18, 20, 36, 38, 42, 47, 49 and 54, and  $\zeta = 347 \pm 3$  of H. Iwano for samples NTR-8, 19, 45, 46, 52, 66, 67, and 71.

Ma, 11.7Ma and 11.6 Ma, respectively, by Potassium-Argon chronostratigraphy in the Karasuyama area, about 190 km southward of the present area, in central Honshu, Japan (Hayashi and Takahashi, 2002). With respect to the above numerical ages, the interval between samples NM-1 and NM-43 should be younger than planktonic foraminiferal zone N.10 of Blow (1969) and M7 of Berggren *et al.* (1995). The interval between sample NH-25 and NH-41 corresponds to zone N.14 of Blow (1969) and M11 of Berggren *et al.* (1995).

### 6.3 Diatoms

*Denticulopsis praedimorpha* var. *praedimorpha* occurs continuously in the upper Hatatate Formation from the 147-m to 194-m level in Fig. 6, indicating that the interval is assigned to the *D. praedimorpha* Zone (NPD 5B) of Akiba's (1986) Neogene North Pacific diatom zonation. Furthermore, the presence of *D. praedimorpha* var. *praedimorpha* without *Crucidentricula nicobarica* places this interval between biohorizons D53 (12.2 Ma) and D 55 (11.4 Ma) of Yanagisawa and Akiba

(1998) and Watanabe and Yanagisawa (2005).

## 7. Discussion

### 7.1 Depositional age Tsunaki and Aoba Sections

The lower unit of the Tsunaki Formation ranges about 10 Ma to 9 Ma in age, with the exception of Sample TS-2 (8.3 $\pm$ 0.4Ma). The basal part of the middle unit of the Tsunaki Formation is assigned to 9 - 8.5 Ma. The upper unit of the Tsunaki Formation was deposited around 8.3 Ma. The basal part of the Nashino Formation is placed around 6.4 Ma.

### Natori-gawa Section

All age data obtained from the Natori-gawa Section are shown in Fig 7. A sediment accumulation curve considering the positive age data is also shown in the figure. The older FT age group in the Hatatate Formation is generally concordant with the biohorizons of the planktonic foraminifers. These age data indicate that the

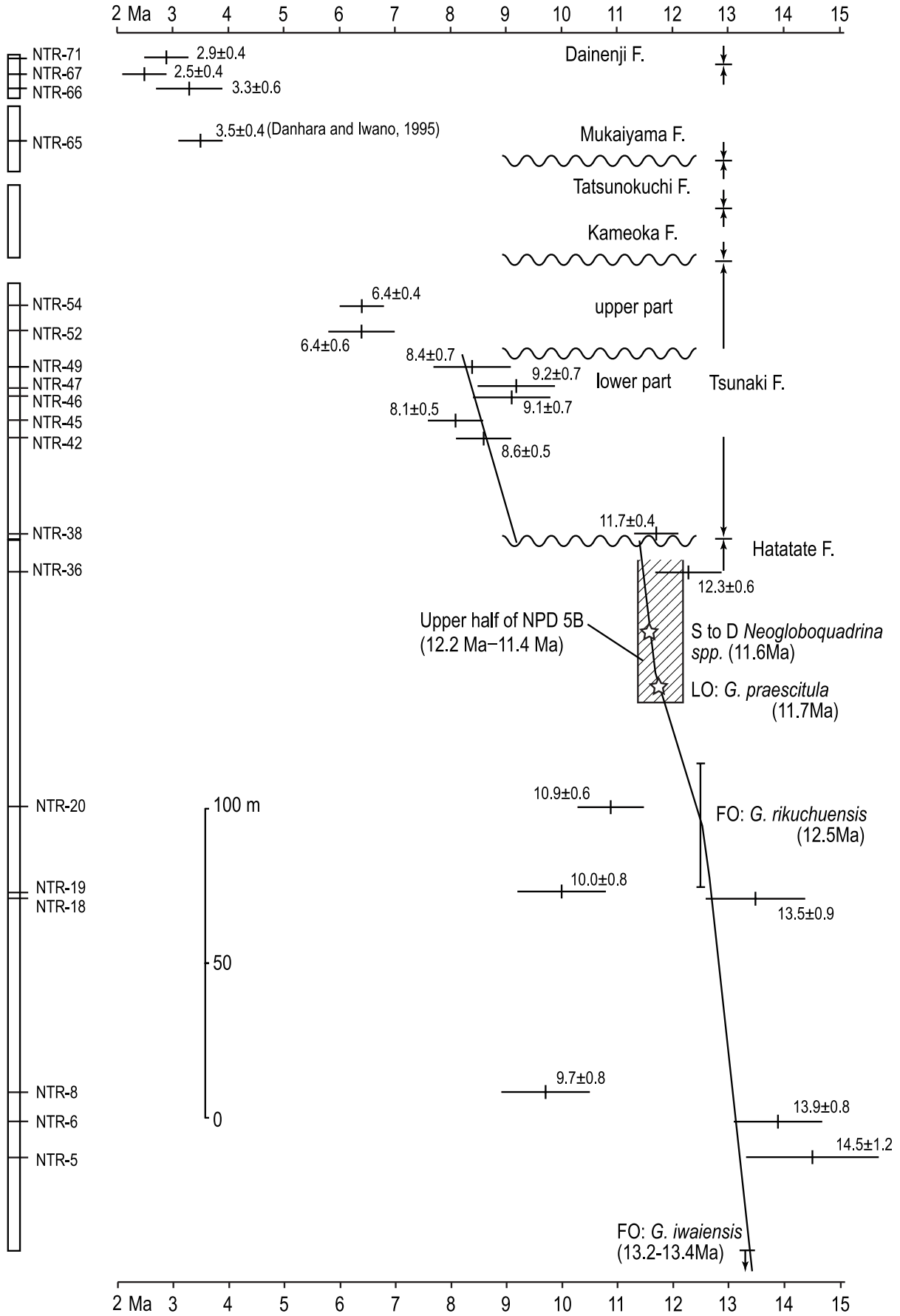


Fig. 7 Summary of chronologic data and sediment accumulation curve for the Natori-gawa Section.

Hatatate Formation cropping out along the present section ranges in age from 13.2 Ma to 11.6 Ma, overall.

The lower part of the Tsunaki Formation in the present section approximately ranges from 9 to 8 Ma in age. This time range and lithofacies are close to those of the middle unit of the Tsunaki Formation in the Tsunaki and Aoba Sections. The FT age of the upper part of the Tsunaki Formation, ~6.4 Ma, is close to the age of the basal part of the Nashino Formation in the Aoba Section. The relationship between the upper part of the Tsunaki Formation in the Natori-gawa Section and the Nashino Formation is unclear.

The FT ages from the Mukaiyama (~3 Ma) and Dainenji ( $2.9\pm 0.4$ ) formations are concordant with the age of the Hirosegawa Tuff Member ( $3.5\pm 0.4$  Ma) intercalated in the lower part of the Mukaiyama Formation.

### 7.2 Ages of major unconformities

Many researchers have reported three major unconformities in the Late Miocene to Pliocene sequence around the Sendai Area (*e.g.* Kitamura *et al.*, 1986). These unconformities bound the Natori, Akiu and Sendai Groups and the lower and upper parts of the Sendai Group (Fig. 2). On the basis of age and lithofacies data in the study area, we recognize another major unconformity between the Tsunaki and Hatatate formations in the Natori-gawa Section (Fig. 7). The uppermost part of the Hatatate Formation and the lower unit of the Tsunaki Formation observed in the Tsunaki and Aoba Sections are absent in the Natori-gawa Section. This unconformity is estimated to have formed around 9 Ma.

We also obtained a numerical age for the unconformity between the Natori and Akiu formations. Age data from the Aoba and Natori-gawa Sections indicate that this unconformity formed in the period of 8.3 Ma to 6.4 Ma. The unconformity between the Akiu and the lower part of the Sendai Group was assigned to the latest Miocene, on the basis of age data from the Tatsunokuchi Formation (Yanagisawa, 1990) and Nashino Formation in the Aoba Section. The unconformity bounding the lower and upper part of the Sendai Group formed around 3.5 Ma, just before deposition of the Hirosegawa Tuff Member.

### 7.3 Relationship between formation of unconformities and uplift of the Ou Backbone Range

The timing of the four unconformities in this study does not always correspond to a trend in eustatic sea-level changes (*e.g.* Haq *et al.*, 1988). They reflect not only eustatic sea-level change but also regional tectonic movement. Sato (1994) reconstructed the tectonic evolution of the Northeast Japan Arc during the late Cenozoic on the basis of a compilation of geological data. He estimated that the Ou Backbone Range started to uplift around 10 Ma, and that the Northeast Honshu Arc has been under an E-W trend crustal shortening defor-

mation regime since 3.5 Ma. Nakajima *et al.* (2006) discussed the Late Cenozoic uplift history of the sedimentary basin in the axial part of the Ou Backbone Range. They identified three stages of uplift under a compressional stress regime, 12-9 Ma, 6.5-3.0 Ma and 3 Ma, mainly based on the temporal and spatial distribution of major unconformities in the Mio-Pliocene sequence.

The unconformities recognized on the southwestern margin of the Sendai Plain broadly correspond to unconformities reported by Nakajima *et al.* (2006) and are interpreted to reflect the uplift history of the Northeast Honshu Arc.

## 8. Conclusions

We obtained following new insights into the chronostratigraphy of the Middle Miocene to Pliocene sequence on the southwestern margin of the Sendai Plain, northeast Japan, on the basis of 27 FT ages in combination with planktonic foraminiferal and diatom analyses.

1. The Hatatate Formation cropping out in the Natori-gawa Section approximately ranges from 13 Ma to 11.5 Ma in age.
2. Numerical age of the Tsunaki and Nashino formations were first revealed by the present study. The Tsunaki Formation ranges from 10 Ma to 8.3 Ma in age, and the basal part of the Nashino Formation is assigned to 6.4 Ma.
3. Four major unconformities are recognized in the Middle Miocene to Pliocene sequence in the study area from a compilation of chronological data, with ages of ca. 9 Ma, 6.4 Ma, latest Miocene, and 3.5 Ma. The oldest unconformity is newly identified in the present study.
4. The formative times of these unconformities serve to constrain the reconstruction of uplift history of the Northeast Honshu Arc.

## Reference

- Akiba, F. (1986) Middle Miocene to Quaternary diatom biostratigraphy in the Nankai Trough and Japan Trench, and modified Lower Miocene through Quaternary diatom zones for middle-to-high latitudes of the North Pacific. In Kagami, H., Karig, D.E., Coulbourn, W.T. *et al.*, *Init. Repts. Deep Sea Drilling Project*, U.S. Govt. Printing Office, Washington D.C., **87**, 393-480.
- Berggren, W. A., Kent, D. V., Swisher, C. C. III and Aubry, M.-P. (1995) A revised Cenozoic geochronology and chronostratigraphy. In Berggren, W. A., Kent, D. V., Aubry, M.-P. and Hardenbol, J., *eds.*, *Geochronology, Time Scales and Global Stratigraphic Correlation*. (SEPM Special Publication, no. 54), 129-212.
- Blow, W. H. (1969) Late middle Eocene to Recent plank-

- tonic foraminiferal biostratigraphy. In Brönnimann, P. and Renz, H. H., eds., *Proceedings of the First International Conference on Planktonic Microfossils, Geneva, 1967*, Leiden E. J. Brill, **1**, 199-421.
- Danhara, T. and Iwano, H. (1995) Fission-track dating of the pyroclastic flow deposit: A case study of the Pliocene Hirosegawa Tuff Member of the Sendai Group in Northeast Honshu, Japan. *Fission Track News Letter*, no.8, 25-34. (in Japanese)
- Danhara, T., Iwano, H., Yoshioka, T. and Tsuruta, T. (2003) Zeta calibration values for fission track dating with a diallyl phthalate detector. *Jour. Geol. Soc. Japan*, **109**, 665-668.
- Danhara, T., Kasuya, M., Iwano, H. and Yamashita, T. (1991) Fission-track age calibration using internal and external surfaces of zircon. *Jour. Geol. Soc. Japan*, **97**, 977-985.
- Galbraith, R. F. (1981) On statistical models for fission track counts. *Jour. Math. Geol.*, **13**, 471-478.
- Haq, B. U., Hardenbol, J. and Vail, P. R. (1988) Mesozoic and Cenozoic chronostratigraphy and eustatic cycles. In Wilgus, C.K., Hastings, B.S., Kendall, G. C. St. C., Posamentier, H., Ross, C. A. and Van Wagonar, J. C., eds., *Sea-level Changes: an Integrated Approach*. (SEPM Special Publication no. 42), 71-108.
- Hayashi, H. and Takahashi, M. (2002) Planktonic foraminiferal biostratigraphy of the Miocene Arakawa Group in central Japan. *Revista Mexicana de Ciencias Geologicas*, **19**, 190-205.
- Hurfurd, A. J. (1990a) Standardization of fission track dating calibration: Recommendation by the Fission Track Working Group of the I. U. G. S. Subcommittee of Geochronology. *Chem. Geol.*, **80**, 171-178.
- Hurfurd, A. J. (1990b) International Union of Geological Sciences Subcommittee on Geochronology recommendation for the standardization of fission-track dating calibration and data reporting. *Nucl. Tracks Radiat. Meas.*, **17**, 233-236.
- Kitamura, N., Ishii, T., Sangawa, A. and Nakagawa, H. (1986) *Geology of the Sendai District*. With geological sheet map at 1:50,000, Geol. Surv. Japan, 134p. (in Japanese with English abstract)
- Nakajima, T., Danhara, T., Iwano, H. and Chinzei, K. (2006) Uplift of the Ou Backbone Range in Northeast Japan around 10 Ma and its implication for the tectonic evolution of the eastern margin of Asia. *Palaeogeogr., Palaeoclim., Palaeoecol.*, **241**, 28-48.
- Oda, M., Hasegawa, S., Honda, N., Maruyama, T. and Funayama, M. (1984) Integrated biostratigraphy of planktonic foraminifera, calcareous nannofossils, radiolarians and diatoms of Middle and Upper Miocene sequences of Central and Northeast Honshu, Japan. *Palaeogeogr., Palaeoclimatol., Palaeoecol.*, **46**, 53-69.
- Ogasawara, K. and Masuda, K. (1989) Paleobathymetric indexes of the Neogene molluscs in Tohoku District and their implications. *Memoirs of the Geol. Soc. Japan*, no. 32, 217-227. (in Japanese with English abstract)
- Okada, H. and Bukry, D. (1980) Supplementary modification and introduction of code numbers to the low-latitude coccolith biostratigraphic zonation (Bukry, 1973, 1975). *Mar. Micropaleont.*, **5**, 321-325.
- Osozawa, S. (2002) Formative process of the Kagitori-Ayashi Line (Monocline) and the Aoba Fault Zone, at the Moniwa and Aobayama hills, Sendai, northeast Japan. *Jour. Geol. Soc. Japan*, **108**, 781-793. (in Japanese with English abstract)
- Sato, H. (1994) The relationship between late Cenozoic tectonic events and stress field and basin development in northeast Japan. *Jour. Geophys. Res.*, **99**, B11, 22261-22274.
- Shimamoto, M., Ota, S., Hayashi, H., Sasaki, O. and Saito, T. (2001) Planktonic foraminiferal biostratigraphy of the Miocene Hatatate Formation in the southwestern part of Sendai City, Northeast Japan. *Jour. Geol. Soc. Japan*, **107**, 258-268. (in Japanese with English abstract)
- Watanabe, M. and Yanagisawa, Y. (2005) Refined Early to Middle Miocene diatom biochronology for the middle- to high-latitude North Pacific. *Island Arc*, **14**, 91-101.
- Yanagisawa, Y. (1990) Diatom biostratigraphy of the Neogene Sendai Group, northeast Honshu, Japan. *Bull. Geol. Surv. Japan*, **41**, 1-22. (in Japanese with English abstract)
- Yanagisawa, Y. (1999) Diatom biostratigraphy of the Middle Miocene Hatatate Formation, Sendai City, Miyagi Prefecture, Japan. *Bull. Geol. Surv. Japan*, **50**, 269-277. (in Japanese with English abstract)
- Yanagisawa, Y. and Akiba, F. (1998) Refined Neogene diatom biostratigraphy for the northwest Pacific around Japan, with an introduction of code numbers for selected diatom biohorizons. *Jour. Geol. Soc. Japan*, **104**, 395-414.
- Yanagisawa, Y. and Hayashi, H. (2003) Marine diatom biostratigraphy and biohorizons of the middle Miocene in Ichinoseki area, Iwate Prefecture, northeastern Japan. *Bull. Geol. Surv. Japan*, **54**, 49-61. (in Japanese with English abstract)

Received July, 15, 2008

Accepted September, 16, 2008

仙台平野南西部に露出する中部中新統 - 鮮新統の年代データ：奥羽脊梁山地の隆起と関連して

藤原 治・柳沢幸夫・入月俊明・島本昌憲・林 広樹・植原 徹・布施圭介・岩野秀樹

要 旨

仙台平野南西部の3つの地質セクションから得られた中部中新統 - 鮮新統の年代層序データを報告する。ここで報告する27個のFT年代測定値と浮遊性有孔虫化石および珪藻化石の分析結果は、調査地域周辺のテクトニックな変動の復元に貢献する。名取川下流の河床に露出する旗立層は地質年代として、ほぼ13 Maから11.5 Maに相当する。綱木層はほぼ10 Maから8.3 Maの期間に堆積した地層であり、梨野層下部は6.4 Ma頃に堆積した。年代と層相のデータを総合すると、この中部中新統 - 鮮新統には4つの比較的大きな不整合が認められる。それらは9 Ma頃、6.4 Ma頃、最後期中新世、および3.5 Ma頃である。最も古い不整合は本研究で新たに見出された。これらの不整合の形成時期は、Nakajima *et al.* (2006) が復元した奥羽脊梁山地の段階的な隆起の歴史と良く対応する。本研究で示したデータは、東北本州弧の隆起時期のより詳しい推定を可能にする。